Sensing and Bio-Sensing Research 7 (2016) 1–6

Contents lists available at ScienceDirect

Sensing and Bio-Sensing Research

journal homepage: www.elsevier.com/locate/sbsr

Design and numerical analysis of microstructured-core octagonal photonic crystal fiber for sensing applications

Kawsar Ahmed *, Monir Morshed

Department of Information and Communication Technology, Mawlana Bhashani Science and Technology University, Santosh, Tangail-1902, Bangladesh

ARTICLE INFO

Article history:
Received 3 July 2015
Received in revised form 18 October 2015
Accepted 20 October 2015

Keywords:
Photonic Crystal Fiber (PCF)
Octagonal photonic crystal fiber (O-PCF)
Evanescent field
Chemical sensor
Sensitivity and confinement loss

ABSTRACT

This paper presents an octagonal photonic crystal fiber (O-PCF) for liquid sensing, in which both core and cladding are microstructured. Some propagation characteristics of proposed structure have been investigated by using the full vectorial finite element method (FEM). Confinement loss and sensitivity are examined and compared with varying number of rings, core diameter, diameter of air holes in cladding ring and pitch. It is found that sensitivity is increased for the increment pitch value, air filling ratio, core diameter, inner ring diameter as well as number of rings. At the same time confinement loss is significantly decreased. It is also found that the increment of pitch by keeping the same air filling ratio increases the sensitivity and loss. Investigating the effects of different parameters, an O-PCF structure is designed which has a significantly higher relative sensitivity and lower confinement loss.

1. Introduction

Larger application areas of Photonic Crystal Fiber (PCF) technologies have attracted much attention in recent years. PCFs have started a new era overcoming many limitations of conventional optical fiber. In the history of optical technology, PCFs have added new epoch through designing freedom [1]. For enormous optical applications, PCFs have been appointed as one of the most fascinating structures [2–3]. Fibers can be categorized in two parts according to guiding mechanism of light. One is effective index guidance PCF that is solid cored and in the cladding area air holes are randomly or periodically [4–5] arranged. In index guiding PCFs air holes at cladding area have a lower effective refractive index compare to a solid core. Another one is photonic-band-gap (PBG) guidance PCF that is capable to control the light guidance for any frequency band. Here light confinement has occurred in the lower indexes core region compare to cladding. A sophisticated device that converts the light rays into electrical signals which can detect the change and response of ambient condition or can measure the intensity of electromagnetic waves called an optical sensor.

PCF technology allows for the accurate tuning of the propagation properties of fiber through changing of air hole shape, size and their positions. Various guiding properties of PCF can be achieved by changing geometry parameters [6]. At PCF, sensing is the interaction between passing light and analyte which are alterable by varying the frequency, intensity, wavelength, phase and polarization state of light etc. [7]. In this respect, PCFs can be designed for sensing applications in environment, biomedical and industry sectors. Better guiding properties have already been achieved by applying different geometric shape lattice structures such as Hexagonal [8], Octagonal [9], Decagonal [10], Elliptical [11] and Circular honey comb cladding [12]. A photonic crystal fiber demonstrates its potentiality for sensing applications due to its unique geometrical structure.

The evanescent wave based PCF sensors are increasing rapidly in chemical and biomedical applications for their attractive features. Besides sensing applications, PCFs are also designed for their extraordinary performance in dispersion [1], birefringence [13], guiding of light in air [14], and nonlinear effect enhancement [15,16] compare to conventional fibers. Higher sensitivity and smaller size have mainly increased the popularity of PCF sensors. However, hollow core PBG PCFs with low relative refractive index gas or chemical at the core region [17–18], are desirable in sensing [17–19]. But the complexity of the manufacturing process is responsible for decrement of PBG PCF applications and increment of index guiding PCF applications in sensing. The evanescent field of PCFs is commonly involved in gas sensing with different index materials [20–24], chemical and bio sensing [25–26]. On the other hand, they are also used as bacteria and remote sensors.

Sensitivity and confinement loss are two key guiding properties of PCF chemical sensors. Several papers have been published to gain sensitivity at a maximum and confinement loss at a minimum satisfactory level in chemical or gas sensing applications. 13.23% sensitivity has been gained by increasing inner ring air hole diameter and also reduced confinement loss to 3.77×10^{-6} dB/m at $\lambda = 1.33$ μm [27]. But M. Morshed et al. [28] improved sensitivity 13.94% compared to [29]. After that, they also gained sensitivity 20.10% for simple PCF structure

* Corresponding author.
E-mail addresses: kawsar.ict@mbstu.ac.bd, kawsarit08050@gmail.com, kawsar_it08050@yahoo.com (K. Ahmed), monirmorshed.mbstu@gmail.com, monirmorshed.ict@mbstu.ac.bd (M. Morshed).

http://dx.doi.org/10.1016/j.sbsr.2015.10.005

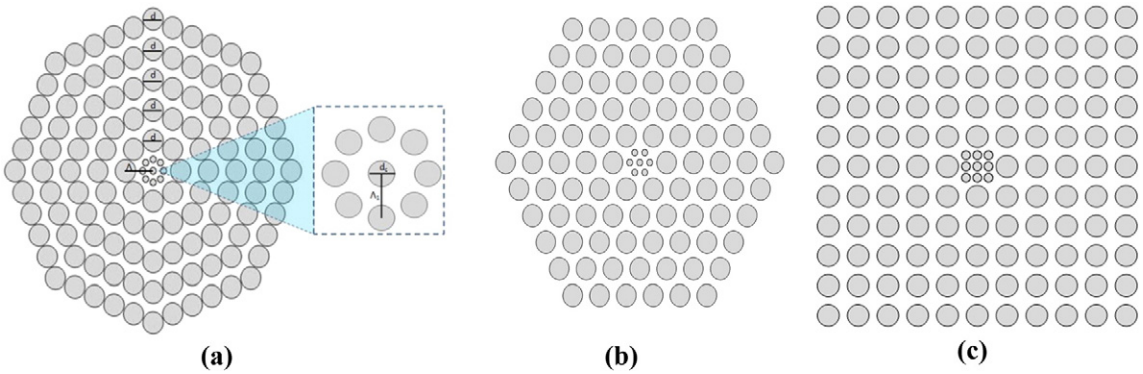

Fig. 1. Designing views of different PCFs geometrical formation (a) O-PCF (b) H-PCF and (c) S-PCF with structural parameters: diameter of air holes in core (d_c), Pitch in core (Λ_1), diameter of air holes in cladding (d) and Pitch in cladding (Λ).

and proved the benefits of modified PCF structure [30]. An index guiding nanostructure PCF has been proposed by S. Olyaee et al. [31] and achieved lower dispersion, confinement loss and nonlinear effect simultaneously. The article [32] improved sensing capacity by developing a new concept for evanescent sensing application in which both core and cladding are microstructured. The article [33] presented that Octagonal PCF shows smaller loss and the higher relative sensitivity coefficient compared with the Hexagonal PCF structure, in which both core and cladding are microstructured and also improved sensitivity by 47% compared to [32] for three analytes like Water, Ethanol and Benzyne. In this paper, it is proposed that an O-PCF structure with high relative sensitivity and low confinement loss compare to [33] as well as two other structures like H-PCF, S-PCF and investigated the effects of different parameter variations on propagation properties over a wide wavelength range.

2. Geometries of proposed O-PCF

The cross sectional views of the proposed O-PCF, S-PCF and H-PCF have been shown in Fig. 1. The figure clearly depicts the whole geometrical structure of the PCF. The proposed structures of the PCF are in square, hexagonal and octagonal shapes. So the vertices of the adjoining air holes contain 45° and 60° angles to form octagonal and hexagonal structures respectively. The hole to hole space (pitch) in cladding has been denoted by Λ for all types of fibers and operations. The diameters of air holes in each ring of cladding are denoted by d. Pure silica has been utilized as the background material for all types of fibers and refractive index is selected using Sellmeier equation [34]. The microstructure core of O-PCF and S-PCF contains 8 holes and H-PCF contains 6 holes. In addition, all fibers have a center air hole. In perspective to all shaping fibers, the diameter of the supplementary air holes in the core region is d_c and the pitch among the supplementary air holes at the core is Λ_1. Various analytes with refractive index like Water (n = 1.33), Ethanol (n = 1.354) and Benzyne (n = 1.366) [35] are filled in the supplementary air holes in the core region. Modal intensity distribution of proposed O-PCF, H-PCF and S-PCF has been shown in Fig. 2 respectively.

3. Synopsis of numerical method

For electromagnetic simulation, the Finite Element Method (FEM) has been utilized for the proposed PCF. Using the Finite Element Method (FEM) two key properties such as sensitivity and confinement loss have been investigated.

The guided light penetrates into the cladding region from the core due to finite number of air holes and it is known as confinement loss. The confinement loss L_c can be calculated through the imaginary part of the refractive index n_{eff} [36]:

$$L_c = \frac{40\pi.\mathrm{IM}[n_{eff}] \times 10^6}{\lambda.\ln(10)}(\mathrm{dB/m}) \tag{1}$$

where, Im $[n_{eff}]$ is known as the imaginary part of the refractive index and λ is the wavelength of light. The interaction between light and the analyte can be measured by the relative sensitivity coefficient and it can be obtained through the following equation [28]:

$$r = \frac{n_r}{n_{eff}} f \tag{2}$$

where, the refractive index of sensed material within the air holes is represented by n_r and the modal effective index is n_{eff}. The ratio of air hole power and the total power percentage can be calculated through

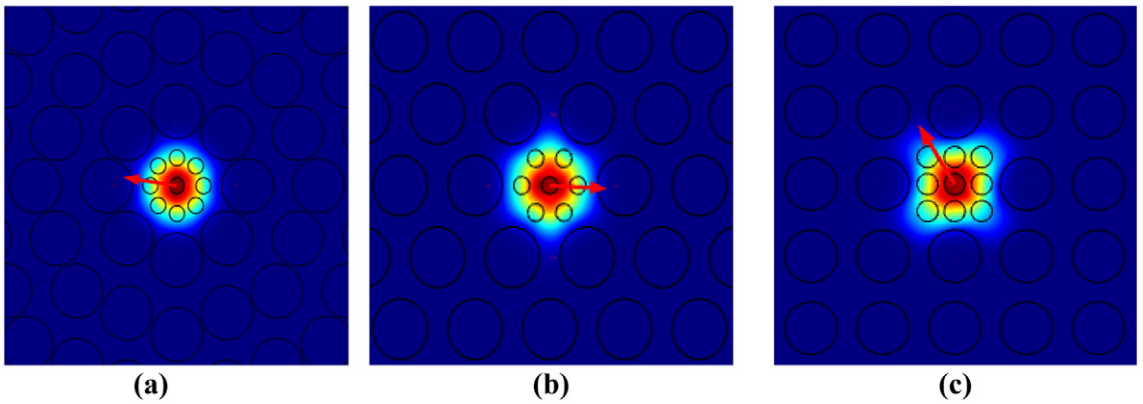

Fig. 2. Modal intensity distribution of proposed (a) O-PCF, (b) H-PCF and (c) S-PCF for Λ = 2.4 μm, d = 1.75 μm, Λ_1 = 0.9 μm, d_c = 0.63 μm, and n = 1.33 at the wavelength of 1.33 μm.

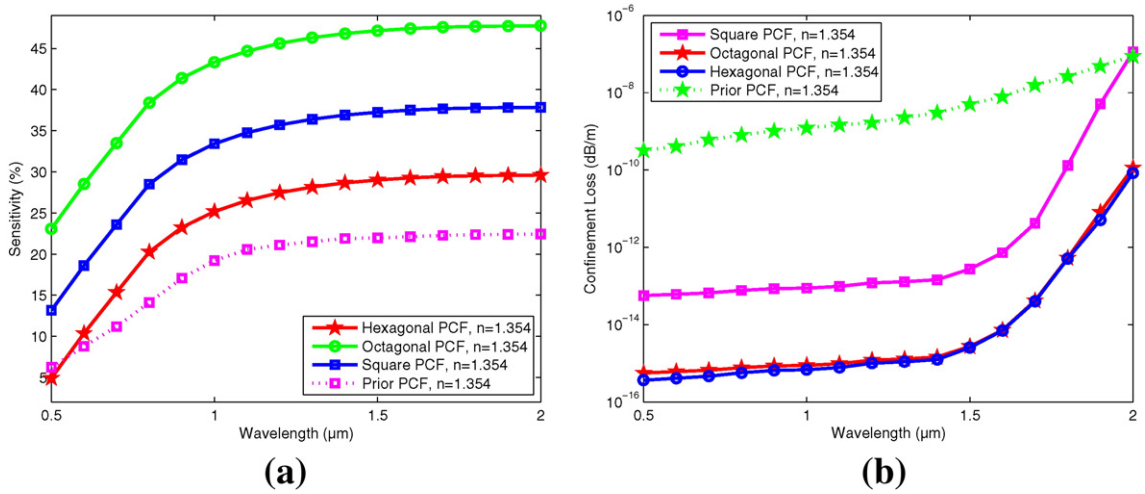

Fig. 3. Comparison of (a) relative sensitivity (%) and (b) confinement loss (dB/m) for different types of PCFs (O-PCF, H-PCF, S-PCF and Prior PCF) keeping all parameters fixed to ˆ = 2.4 μm, d = 1.75 μm, ˆ1 = 0.9 μm, and d_c = 0.63 μm.

Eq. (3) and represented by *f*:

$$f = \frac{\int_{sample} Re(E_x H_y - E_y H_x)\,dxdy}{\int_{total} Re(E_x H_y - E_y H_x)\,dxdy} \times 100 \quad (3)$$

where, E_x and H_x are transverse electric field and magnetic field, E_y and H_y are longitudinal electric field and magnetic field respectively. The mode field pattern E_x, H_x, E_y , H_y and effective index n_{eff} have been obtained by applying the finite-element method (FEM).

4. Results and numerical analysis

The proposed PCF supports the fundamental mode as well as some higher order mode. But here it is considered as a fundamental mode for further investigation of propagation characteristics. A comparison among O-PCF, H-PCF, S-PCF and Prior PCF is shown in Fig. 3 for the optimized parameters: ˆ = 2.4 μm, d = 1.75 μm, ˆ1 = 0.9 μm and d_c = 0.63 μm.

From Fig. 3 (a) it is clearly visualized that O-PCF shows the higher sensitivity compare to H-PCF, S-PCF and Prior O-PCF [33]. At the wavelength of 1.33 μm, O-PCF has the sensitivity of 46.31% whereas H-PCF, S-PCF and prior O-PCF show the sensitivity of 28.16%, 36.39%, and 21.50%, respectively. At the same time O-PCF shows the lowest confinement loss which is shown in Fig. 3 (b). So Octagonal PCF is chosen and proposed in this paper.

A simple technique has been applied to optimize the parameters. In the proposed structure the thickness is fixed at 10% of the radius of the proposed fiber by PML test for efficient calculation of confinement loss following M. Morshed et al.'s article [37]. But no significant effect on the relative sensitivity has been observed here. The thickness of circular PML is selected by 1.5 μm. COMSOL Multiphysics 4.2 is used here for simulating the proposed O-PCF by selecting Fine mode of Mesh size. Defective modes in PCF with compactly supported perturbations are known as convergence error. The convergence error of our proposed O-PCF is very low at about 5.8×10^{-6}%. Firstly, the effects of rings are investigated which is shown in Fig. 4.

Under the same criterion of the different parameters (ˆ = 2.4 μm, d = 1.75 μm, ˆ1 = 0.9 μm, d_c = 0.63 μm) the confinement loss and sensitivity of O-PCF structures with different ring numbers have been investigated and compared in Fig. 4 (a) and (b).The sensitivity for rings 6, 5, 4, and 3 is 47.74%, 47.67%, 45.32% and 43.78%; confinement loss is 1.00497×10^{-15}; 1.29497×10^{-15} dB/m, 1.75918×10^{-15} dB/m and 2.75918×10^{-14} respectively at λ = 1.33 μm. 6-ring O-PCF shows the lowest confinement loss compare to all O-PCFs but quite similar to 5-ring O-PCF. For 5-ring O-PCF, sensitivity is also quite similar with the 6th, 7th and 8th-ring of O-PCF. Although, we have shown up to 6 ring O-PCF in Fig. 4. So for further investigation process 5-ring O-PCF is

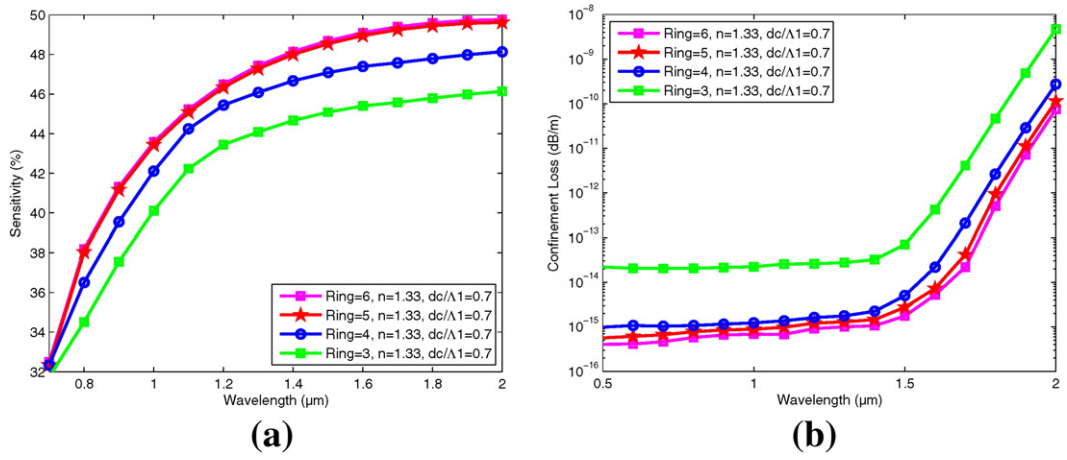

Fig. 4. Comparison of (a) relative sensitivity (%) and (b) confinement loss (dB/m) according to wavelength for a different number of rings while other parameters are kept fixed to ˆ = 2.4 μm, d = 1.75 μm, ˆ1 = 0.9 μm and d_c = 0.63 μm.

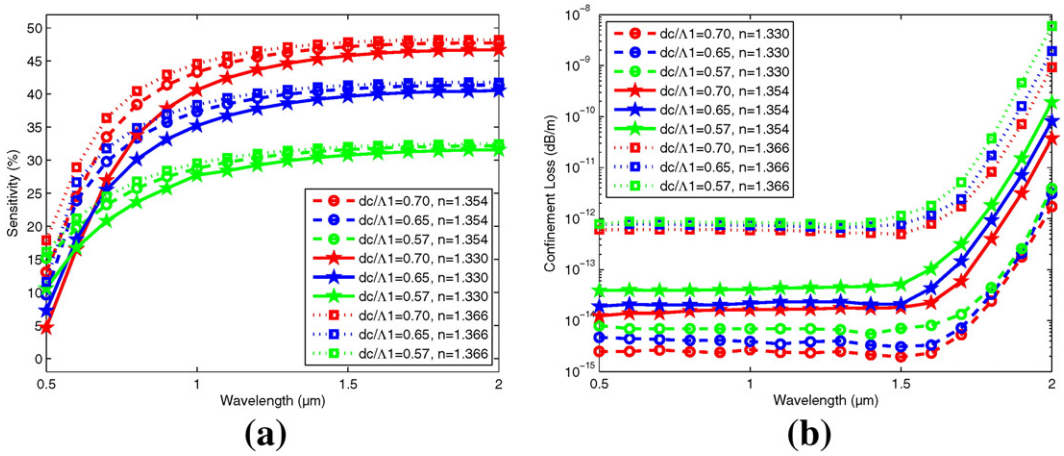

Fig. 5. Comparison of (a) relative sensitivity (%) and (b) confinement loss (dB/m) according to wavelength for different values of air filling ratio (d_c/Λ_1) when other parameters are kept constant to$^{\wedge} = 2.4$ μm, $\Lambda_1 = 0.9$ μm, d = 1.75 μm.

considered for sensing applications to avoid structural complexity and more fabrication cost compare to 6 or higher ring O-PCF.

In Fig. 5 (a), the sensitivity of the proposed PCF is greatly enhanced by the increasing air filling ratio. Air filling ratio (d_c/Λ_1) is varied by 0.70, 0.65 and 0.57 and the calculated sensitivity at $\lambda = 1.33$ μm is 44.63, 38.61 and 29.91% respectively; the confinement loss is 2.477×10^{-15}, 4.021×10^{-13} and 6.636×10^{-15} dB/m respectively for Water. At a core diameter $d_c = 0.63$ μm, the proposed O-PCF shows better propagation characteristics for Water, Ethanol and Benzyne analytes at $\lambda = 1.33$ μm; the calculated sensitivity is 44.73%, 46.67%, and 47.35%; and the confinement loss is 3.897×10^{-15}, 6.266×10^{-15}, and 2.282×10^{-14} dB/m respectively. From Fig. 5, it is acquitted that sensitivity increases by the increment of air filling ratio and confinement loss is vice versa. So another optimal parameter $d_c = 0.63$ μm of 5-ring O-PCF is chosen for further investigation.

Fig. 6 (a) and (b) depicts the sensitivity and confinement loss of the proposed fiber for the pitch (Λ_1) variation keeping air filling ratio (d_c/Λ_1) constant. Three pitches ($\Lambda_1 = 0.7$, 0.8 and 0.9 μm) are considered and $^{\wedge} = 2.4$ μm and d = 1.75 μm remain unchanged. Now keeping the air filling ratio fixed, the pitch (Λ_1) and core diameter (d_c) are varied. It is evident from Fig. 6 that the highest sensitivity and lowest confinement loss are shown at $\Lambda_1 = 0.9$ μm and $d_c = 0.63$ μm for all analytes. So for better propagation characteristics, core pitch value of 0.9 μm is recommended here for further investigation procedure.

Fig. 7 (a) and (b) illustrates the scenario of changing sensitivity and confinement loss of proposed O-PCF as the variation of the inner most ring air hole diameters for $^{\wedge} = 2.4$ μm, $d_c/\Lambda_1 = 0.7$, and $\Lambda_1 = 0.9$ μm. The relative sensitivities at $\lambda = 1.33$ μm for d = 1.75 μm, 1.68 μm and 1.60 μm are 47.58%, 44.93%, 42.85%; 48.73%, 46.51%, 44.45% and 49.97%, 47.31%,45.22% for Water, Ethanol and Benzyne analytes respectively. In order to support the numerically investigated results represented in Fig. 7 (a), by increasing the diameter of the inner most air holes the sensitivity can be greatly enhanced. One remarkable reason is from Fig. 7 (b) which states that confinement loss is dramatically unchanged. The confinement loss for the proposed O-PCF is 2.47705×10^{-15}, 2.67705×10^{-15}, and 2.27705×10^{-15} dB/m; 2.07451×10^{-14}, 2.37451×10^{-14}, and 1.77451×10^{-14} dB/m; 7.58542×10^{-14}, 7.88542×10^{-14} and 7.18542×10^{-14} dB/m for Water, Ethanol, and Benzyne analytes respectively keeping other parameters constant like Fig. 7(a).

After all, confinement loss and the effective refractive coefficient have been studied in this research. All numerically investigated results have shown that relative sensitivity is greatly enhanced due to the high value of the inner most air hole diameters, air filling ratio, pitch, center core diameters as well as number of rings. Highest sensitivity proves more confinement of light in core region as well as the higher electromagnetic power interaction between light and the analytes. From the observation of all results it can be also visualized that the increment of sensitivity and wavelength is shaped. This phenomenon highlights the significant interaction between analytes and light at higher wavelengths.

Almost all sensing applications, higher sensitivity and lower confinement loss through a wide range of wavelength are mostly acceptable

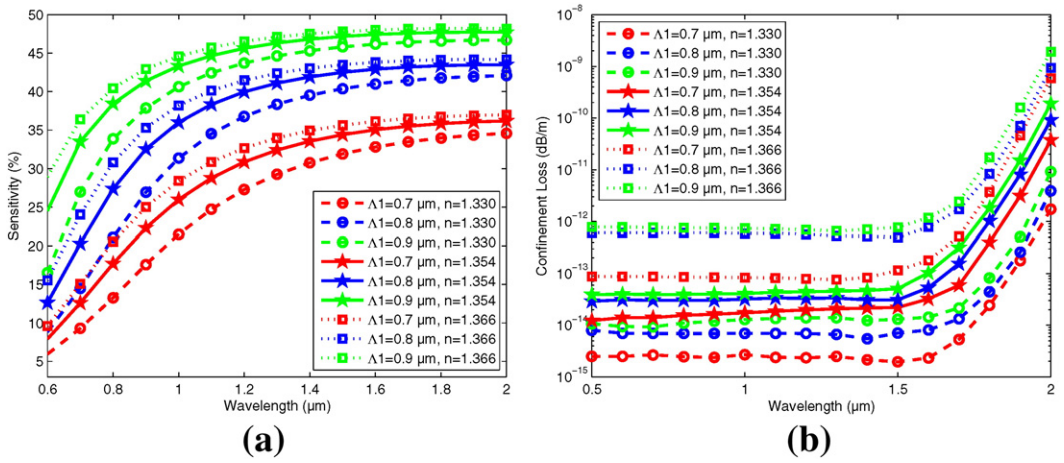

Fig. 6. Comparison of (a) relative sensitivity (%) and (b) confinement loss (dB/m) according to wavelength for different values of Λ_1 when other parameters are kept constant to$^{\wedge} = 2.4$ μm, d = 1.75 μm, and $d_c/\Lambda_1 = 0.7$ μm.

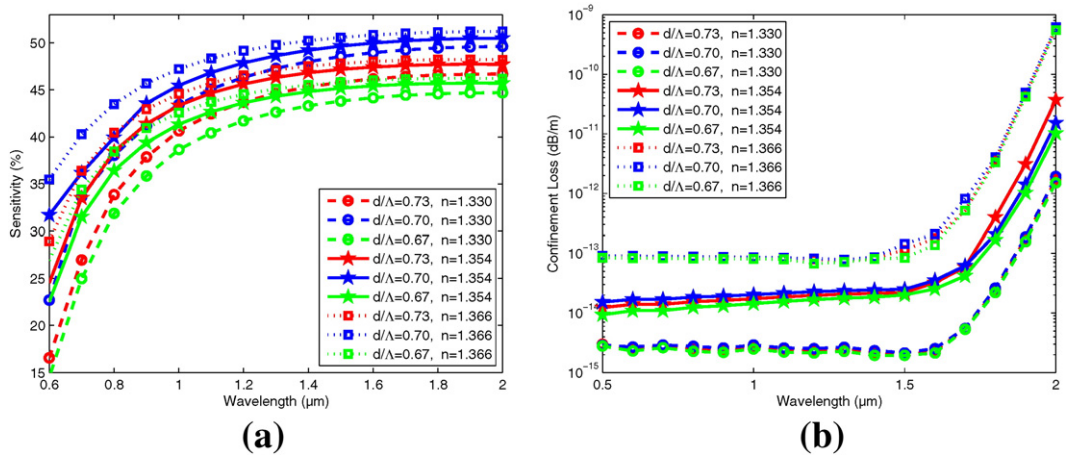

Fig. 7. Comparison of (a) relative sensitivity (%) and (b) confinement loss (dB/m) according to wavelength for different values of the 1st ring air hole diameter (d) by keeping other parameters constant to ˆ = 2.4 μm, $d_c = 0.63$ μm, ˆ$_1$ = 0.9 μm.

essential parameters for designing PCF structure. In this research, it is proved that higher sensitivity and lower confinement loss levels can be gained by the proposed O-PCF compared to previous demonstrated O-PCF structure [33] as well as H-PCF and S-PCF structures. The proposed O-PCF structure's sensitivity has been increased to 45.05%, 46. 87%, 47.35% from 20.05%, 21.55%, 22.50% respectively for all three analytes at $\lambda = 1.33$ μm. Similarly confinement loss is also improved to 6.63622×10^{-15} dB/m, 2.28217×10^{-14} dB/m, 5.28542×10^{-14} dB/m from 5.55×10^{-09} dB/m, 5.65×10^{-09} dB/m, 5.75×10^{-09} dB/m respectively.

Fabrication issues of the proposed O-PCF structure are the most important topic through the experimental point of view. The fabrication process of the proposed O-PCF may not be easy due to micro cored holes. Not only fabrication criteria can be overcome due to technological advancement but also analytes can be entered into the fiber without damages of the fiber's integrity. Several techniques are introduced to fill the air holes with liquid. But the major complexity will be raised in the core region of the proposed structure. The Selective-filling technique was proposed by Huang et al. [38] which is able to fill all cladding holes as well as the micro core holes. Xiao et al. [39] and Cordeiro et al. [40] proposed techniques that were smoothly used to fabricate various PCF structures with liquid at core holes. Lastly the complexity of fabrication will be less due to large air hole diameters and their uniformity with the proposed O-PCF structure [39–40]. Now Sol–gel technique has been applied to remove the complexity of fabrication for any kind of microstructured optical fiber as well as PCF with different types of air hole shapes and sizes [41]. So the proposed PCF can be successfully fabricated using the Sol–gel technique.

5. Conclusion

This paper numerically investigates propagation characteristics of proposed O-PCF, including confinement loss and sensitivity for a wide range of wavelength. The behavior of the proposed PCF for change of different parameters has been also investigated by using Water, Ethanol and Benzyne as analytes. The investigated results indicate that the increment of ring number increases sensitivity until a certain time and confinement loss is vice versa. Better performance of sensitivity and confinement are also shown through the increment of pitch value, air filling ratio, core diameter and inner ring diameter such as increment by ring number. The proposed PCF shows sensitivity: 45.05%, 46. 87%, and 47.35% and confinement loss: 6.63622×10^{-15}, 2.28217×10^{-14}, and 5.28542×10^{-14} dB/m for Water, Ethanol and Benzyne analytes respectively at the wavelength $\lambda = 1.33$ μm. Our proposed O-PCF shows better performance for both sensitivity and confinement loss compared to prior O-PCF [33], H-PCF and S-PCF structures. So, it is affirmed that it could provide new dimension for liquid sensing.

Financial support

No financial support was provided to any of the authors in the creation/writing of this manuscript.

Conflict of interest

The authors declare that they have no competing interests.

Acknowledgment

The authors are grateful to the participants who contributed to this research.

References

[1] W.H. Reeves, D.V. Skryabin, F. Biancalana, J.C. Knight, P.S.J. Russell, F.G. Omenetto, A. Efimov, A.J. Taylor, Transformation and control of ultra-short pulses in dispersion-engineered photonic crystal fibres, Nature 424 (2003) 511–515.
[2] P. Russell, Photonic-crystal fibers, Science 299 (2003) 358–362.
[3] F. Zolla, G. Renversez, A. Nicolet, B. Kuhlmey, S. Guenneau, D. Felbacq, Foundations of Photonic Crystal Fibers, Imperial Collage Press, London, 2005.
[4] J.C. Knight, T.P.S. Birks, J. Russell, D. Atkin, All-silica single-mode optical fiber with photonic crystal cladding, Opt. Lett. 21 (1996) 1547–1549.
[5] A. Bjarkev, J. Broeng, A.S. Bjarkev, Photonic Crystal Fibres, Culver Academic, Boston, 2003.
[6] Z. Xu, K. Duan, Z. Liu, Y. Wang, W. Zhao, Numerical analyses of splice losses of photonic crystal fibers, Opt. Commun. 282 (2009) 4527–4531.
[7] B.Q. Wu, Y. Lu, C.J. Hao, L.C. Duan, N.N. Luan, Z.Q. Zhao, J.Q. Yao, Hollow-core photonic crystal fiber based on C2H2 and NH3 gas sensor, Appl. Mech. Mater. 411 (2013) 1577–1580.
[8] F. Begum, Y. Namihira, S.A. Razzak, S. Kaijage, N.H. Hai, T. Kinjo, K. Miyagi, N. Zou, Design and analysis of novel highly nonlinear photonic crystal fibers with ultra-flattened chromatic dispersion, Opt. Commun. 282 (2009) 1416–1421.
[9] M.S. Habib, M.S. Habib, S.A. Razzak, M.A. Hossain, Proposal for highly birefringent broadband dispersion compensating octagonal photonic crystal fiber, Opt. Fiber Technol. 19 (2013) 461–467.
[10] S.A. Razzak, Y. Namihira, M. Abdul, F. Begum, S. Kaijage, Guiding properties of a decagonal photonic crystal fiber, J. Microw. Optoelectron. 6 (2007) 44–49.
[11] R. Hao, Z. Li, G. Sun, L. Niu, Y. Sun, Analysis on photonic crystal fibers with circular air holes in elliptical configuration, Opt. Fiber Technol. 19 (2013) 363–368.
[12] Y. Hou, F. Fan, Z.-W. Jiang, X.-H. Wang, S.-J. Chang, Highly birefringent polymer terahertz fiber with honeycomb cladding, Opt.-Int. J. Light Electron Opt. 124 (2013) 3095–3098.
[13] A. Ortigosa-Blanch, J.C. Knight, W.J. Wadsworth, J. Arriaga, B.J. Mangan, T.A. Birks, P.S.J. Russell, Highly birefringent photonic crystal fibers, Opt. Lett. 25 (2000) 1325–1327.
[14] R.F. Cregan, B.J. Mangan, J.C. Knight, T.A.P.S. Birks, J. Russell, P.J. Roberts, D.C. Allan, Single-mode photonic band gap guidance of light in air, Science 285 (1999) 1537–1539.

[15] H.E. Heidepriem, P. Petropoulos, S. Asimakis, V. Finazzi, R. Moore, K. Framp-ton, F. Koizumi, D. Richardson, T. Monro, Bismuth glass holey fibers with high nonlinearity, Opt. Express 12 (2004) 5082–5087.
[16] G.P. Agrawal (Ed.), Nonlinear Fiber Optics, 4th ed.Academic Press, San Diego, CA, 2006.
[17] M. Humbert, J.C. Knight, G.P.S. Bouwmans, J. Russell, D.P. Williams, P.J. Roberts, B.J. Mangan, Hollow core photonic crystal fibers for beam delivery, Opt. Express 12 (2004) 1477–1484.
[18] T. Ritari, J. Tuominen, J.C. Petersen, T. Sorensen, T.P. Hansen, H. Simonsen, H. Ludvigsen, Gas sensing using air-guiding photonic bandgap fibers, Opt. Express 12 (2004) 4080–4087.
[19] K.T.V. Grattan, T. Sun, Fiber optic sensor technology: an overview, Sens. Actuators A Phys. 82 (2000) 40–61.
[20] G.A. Cardenas-Sevilla, V. Finazzi, J. Villatoro, V. Pruneri, Photonic crystal fiber sensor based on modes overlapping, Opt. Express 19 (2011) 7596–7602.
[21] C.M.B. Cordeiro, M.A.R. Franco, G. Chesini, E.C.S. Barretto, R. Lwin, C.H.B. Cruz, M.C.J. Large, Microstructured-core optical fibre for evanescent sensing applications, Opt. Express 14 (2006) 13056–13066.
[22] T.M. Monro, W. Belardi, K. Furusawa, J.C. Baggett, N.G.R. Broderick, D.J. Richard-son, Sensing with microstructured optical fibres, Meas. Sci. Technol. 12 (2001) 854–858.
[23] Y.L. Hoo, W. Jin, H.L. Ho, D.N. Wang, R.S. Windeler, Evanescent-wave gas sensing using microstructure fiber, Opt. Eng. 41 (2002) 8–9.
[24] M. Morshed, M.I. Hassan, T.K. Roy, M.S. Uddin, S.M.A. Razzak, Microstructure core photonic crystal fiber for gas sensing applications, Appl. Optics. 54 (2015) 8637–8643.
[25] J.B. Jensen, P.E. Hoiby, G. Emiliyanov, O. Bang, L.H. Pedersen, A. Bjarklev, Selective detection of antibodies in microstructured polymer optical fibers, Opt. Express 13 (2005) 5883–5889.
[26] B.T. Kuhlmey, B.J. Eggleton, D.K.C. Wu, Fluid-filled solid-core photonic band gap fibers, J. Light Wave Technol. 27 (2009) 1617–1630.
[27] S. Olyaee, A. Naraghi, V. Ahmadi, High sensitivity evanescent-field gas sensor based on modified photonic crystal fiber for gas condensate and air pollution monitoring, Opt.-Int. J. Light Electron Opt. 125 (2014) 596–600.
[28] M. Morshed, S. Asaduzzaman, M.F.H. Arif, K. Ahmed, Proposal of simple gas sensor based on micro structure optical fiber, 2nd International Conference on Electrical Engineering and Information & Communication Technology, Bangladesh, 2015.
[29] J. Park, S. Lee, S. Kim, K. Oh, Enhancement of chemical sensing capability in a photonic crystal fiber with a hollow high index ring defect at the center, Opt. Express 19 (2011) 1921–1929.
[30] M. Morshed, M.F.H. Arif, S. Asaduzzaman, K. Ahmed, Design and characterization of photonic crystal fiber for sensing applications, Eur. Sci. J. 11 (2015) 228–235.
[31] S. Olyaee, M. Seifouri, A. Nikoosohbat, M.S.E. Abadi, Low nonlinear effects index-guiding nanostructured photonic crystal fiber, International Journal of Chemical, Nuclear Mater. Metall. Eng. 9 (2015) 253–257.
[32] C. Cordeiro, M.A. Franco, G. Chesini, E. Barretto, R. Lwin, C.H. Brito Cruz, M.C. Large, Microstructured-core optical fibre for evanescent sensing applications, Opt. Express 14 (2006) 13056–13066.
[33] H. Ademgil, Highly sensitive octagonal photonic crystal fiber based sensor, Opt.-Int. J. Light Electron Opt. 125 (2014) 6274–6278.
[34] G. Ghosh, Sellmeier coefficients and dispersion of thermo-optic coefficients for some optical glasses, Appl. Opt. 36 (1997) 1540–1546.
[35] R.C. Kamikawachi, I. Abe, A.S. Paterno, H.J. Kalinowski, M. Muller, J.L. Pinto, J.L. Fabris, Determination of thermo-optic coefficient in liquids with fiber Bragg grating refract meter, Opt. Commun. 281 (2008) 621–625.
[36] M. Pourmahyabadi, S.M. Nejad, Numerical analysis of index-guiding photonic crystal fibers with low confinement loss and ultra-flattened dispersion by FDFD method, Iran. J. Electr. Elect. Eng. 5 (2009) 170–197.
[37] M. Morshed, M.I. Hasan, S.M.A. Razzak, Enhancement of the sensitivity of gas sensor based on microstructure optical fiber, Photonic Sensors (2015) 1-9.
[38] Y. Huang, Y. Xu, A. Yariv, Fabrication of functional microstructured optical fibers through a selective-filling technique, Appl. Phys. Lett. 85 (2004) 5182–5184.
[39] L. Xiao, W. Jin, M. Demokan, H. Ho, Y. Hoo, C. Zhao, Fabrication of selective injection microstructured optical fibers with a conventional fusion splicer, Opt. Express 13 (2005) 9014–9022.
[40] M.B.C. Cordeiro, E.M. dos Santos, C.H.B. Cruz, C.J. de Matos, D.S. Ferreiira, Lateral access to the holes of photonic crystal fibers — selective filling and sensing applications, Opt. Express 14 (2006) 8403–8412.
[41] R.T. Bise, D.J. Trevor, Sol–gel derived microstructured fiber: fabrication and characterization, Opt. Soc. Am. 1-3 (2005).